Title
OBSERVATIONS IN THE REACTION OF TWO DOUBLY-MAGIC NUCLEI: 208Pb AND 48Ca

Author
Nitschke, J.M.

Publication Date
1977-06-01

Submitted to Physical Review Letters

LBL-6534
Preprint c.1

OBSERVATIONS IN THE REACTION OF TWO DOUBLY-MAGIC NUCLEI: ^{208}Pb AND ^{48}Ca

J. M. Nitschke, R. E. Leber, M. J. Nurmia, and A. Ghiorso

June 10, 1977

Prepared for the U. S. Energy Research and Development Administration under Contract W-7405-ENG-48

DISCLAIMER

OBSERVATIONS IN THE REACTION OF TWO DOUBLY-MAGIC NUCLEI: ^{208}Pb AND ^{48}Ca*

J. M. Nitschke, R. E. Leber, M. J. Nurmia, and A. Ghiorso

Lawrence Berkeley Laboratory, University of California
Berkeley, California 94720

ABSTRACT

Excitation functions for compound-nucleus and transfer reactions have beem measured with ^{48}Ca ions on ^{208}Pb targets. A comparison is made with the ^{40}Ar on ^{208}Pb reaction to interpret the observed anomalous behavior of the transfer reactions and a sharp cutoff of the 3n exit channel. Models to interpret these effects are discussed.

Introduction

All attempts to synthesize superheavy elements via nuclear reactions have failed thus far despite efforts to come as close as possible to the predicted island of stability by using for instance the neutron-rich projectile ^{48}Ca to bombard the neutron-rich target ^{248}Cm.[1] Since it is of utmost importance to form superheavy nuclei with as little excitation energy as possible, magic nuclei deserve special consideration. We have chosen the optimum case: the interaction of two doubly magic nuclei ^{208}Pb and ^{48}Ca. Due to the filling of major particle shells ^{208}Pb and ^{48}Ca show shell effects[2] of -10 MeV and -1.1 MeV, respectively which leads in their combination as a compound nucleus to a minimum excitation energy of 26.1 MeV. For the purpose of comparison we have also studied the reaction of ^{208}Pb with ^{40}Ar which has a shell effect of +2.5 MeV and leads to a minimum excitation energy of 36.4 MeV.

EXPERIMENTAL

The experimental technique[3] consists of transporting nuclei in a stream of helium seeded with sodium chloride aerosols through a teflon capillary to the surface of a magnesium wheel which is stepped at a predetermined rate to position the activity spots in front of seven surface barrier detectors. The information obtained from the detectors is processed by a computer. The targets consisted of ^{208}PbO deposited with a thickness of 1 mg/cm^2 on a thin palladium-covered molybdenum foil. PbO was preferred over Pb metal or PbS due to its higher thermal stability. The maximum target temperature was limited through the use of a gas cooling system[4] and monitored by an infrared sensor. Typical beam current densities were 6 $\mu A(electrical)/cm^2$. The details of accelerating Ca ions are described elsewhere.[5]

RESULTS

Excitation functions for the $^{208}Pb(HI,xn)$ reactions and for transfer products in the Bi-Po region were measured and are shown in Fig. 1. The same figure shows the calculated cross sections for the xn exit channels. The calculations were performed with the JORPL code[6] which calculates neutron-evaporation cross sections without explicitly considering de-excitation by γ decay. The following observations are pertinent to the results of the Ar on Pb experiment shown in Fig. 1a.

1. The 3n evaporation product ^{245}Fm is well identified by its half-life of 4.5 ± 0.6s ($T_{1/2}^{lit}$ = 4.2s) and its alpha energy E_α = 8.15 ± 0.02 MeV (E_α^{lit} = 8.15 MeV). Its peak cross section of 15 ± 5nb at 198 MeV agrees well with the calculated value of 18.6 nb (197.5 MeV).

2. The alpha particles of the 2n evaporation product, ^{246}Fm are not observed above a detection limit of 2nb. This result is at variance with the observation of a 1 sec spontaneous-fission activity by Oganessian et al.[7] which was produced with a peak cross section of 7 nb and attributed to the ∿10% SF branching of ^{246}Fm.

3. A 3ms SF activity was observed in a later experiment[8] and is possibly due to the Ar,4n reaction product, ^{244}Fm. All observed cross sections are in agreement with JORPL calculations.

While the ^{40}Ar on ^{208}Pb reaction shows the expected behavior, the ^{48}Ca bombardment (Fig. 1b) displays two striking effects:

1. The onset of the production of the transfer reaction nuclides ^{211}Bi, ^{211m}Po, and ^{212m}Po begins at the same energy as for the the compound-nucleus product, ^{254}No, in sharp contrast to the ^{40}Ar case where their production begins at an energy 10-15 MeV lower than that for the compound-nucleus product, ^{245}Fm.

2. The 3n evaporation product ^{253}No which was expected to be produced with a cross section of 8μb is not observed above a detection limit of 20nb. The 2n evaporation residue ^{254}No is seen with a maximum cross section of 3.4 ± 0.4 μb at 227 MeV

bombarding energy in agreement with findings of Flerov et al.[9] but is in poor agreement with JORPL calculations of 0.45 μb at 223 MeV. Further, the width of the 2n distribution is wider than expected from calculations.

DISCUSSION

Our understanding of the displacement of the tranfer reactions is based on the observation that the same cluster of transferred nucleons is more strongly bound in ^{48}Ca than in ^{40}Ar. A smaller distance between the ^{48}Ca and the ^{208}Pb nucleus is therefore necessary in order to obtain the same transfer probability.

Taking the reaction $^{208}\text{Pb} + 2\text{np} \rightarrow {}^{211}\text{Bi}$ as a representative case, we calculate from experimental masses[10] that the binding energy for the (2np) cluster in ^{48}Ca is 32.23 MeV and in ^{40}Ar 28.67 MeV. Assuming that the probability Ψ^2 of finding a cluster of nucleons outside the nucleus diminishes exponentially with its distance s from the nuclear surface, we have $\Psi^2 \propto \exp(-s/\lambda)$. Where λ is the Compton wavelength of the cluster related to its binding energy E_b and its reduced mass μ via

$$\lambda = \hbar/(2\mu E_b)^{1/2} \quad . \tag{1}$$

We now require that the probability of finding a 2np cluster at the surface of the ^{208}Pb nucleus be independent of whether the cluster originates from a Ca or an Ar nucleus. Schematically $(\Psi^{2np}_{Ca})^2 = (\Psi^{2np}_{Ar})^2$. This leads to the condition:

$$s_{Ca} = s_{Ar} \cdot \lambda_{Ca} / \lambda_{Ar} \tag{2}$$

s_{Ar} can be calculated from the relation $s_{Ar} = R_B - R_o(Pb) - R_o(Ar)$. Here $R_o = r_o A^{1/3}$ and $r_o = 1.07$ fm which corresponds to the point of half-maximum density of the individual nuclei.[11] Since the highest probabality for transfer occurs near or at the top of the barrier, the distance R_B between the centers of the interacting nuclei is obtained from the condition $(dV/dr) = 0$ with $V(r)$ being a suitably chosen interaction potential composed of a coulomb, nuclear, and centrifugal term: $V(r) = V_{coul}(r) + V_{nucl}(r) + V_{centr}(r)$. The first and last terms have the conventional form. For the nuclear potential we have used the proximity force as described in Ref. 12. The resulting potential for $^{40}Ar + ^{208}Pb$ at $\ell = 0$ is shown in Fig. 2a from which we obtain $R_B = 11.95$ fm. This yields $s_{Ar} = 1.95$ fm. From Eq. 1 we obtain for $\lambda^{2np}_{Ca} = 0.468$ fm and $\lambda^{2np}_{Ar} = 0.497$ fm which through application of Eq. 2 results in $s_{Ca} = 1.84$ fm. This has to be compared with s'_{Ca} calculated from $s'_{Ca} = R_B - R_o(Pb) - R_o(Ca)$. Figure 2b shows the $^{48}Ca + ^{208}Pb$ interaction potential with the top of the barrier for $\ell = 0$ being at $R_B = 12.25$ fm which gives $s'_{Ca} = 2.02$ fm. It is now obvious that for $\ell = 0$ the ^{48}Ca nucleus is $\Delta s_{Ca} = s'_{Ca} - s_{Ca} = 2.02 - 1.84 = 0.18$ fm too far away from the Pb nucleus to have a transfer probability for the 2np cluster equal to the $^{40}Ar + ^{208}Pb$ case.* However, as can be seen from Fig. 2b for higher ℓ-waves the top of the barrier E_B is at closer

---

* A comparison between ^{40}Ar and ^{48}Ca made for $\ell > 0$ does not alter the proposed interpretation.

center-to-center distances, to first order with a slope of $\partial E_B/\partial r$ = -58 MeV/fm. Moving the ^{48}Ca and the ^{208}Pb nuclei closer together by Δs_{Ca} = 0.18 fm requires therefore an additional energy of 0.18 × 58 = 10.4 MeV and an angular momentum of about 53 $\hbar$. To visually compare the ^{48}Ca with the ^{40}Ar experiment in Fig. 1., we subtracted 10.4 MeV from the data points for the ^{48}Ca reaction, multiplied the result by the ratio of the interaction barriers 162.5/179.9 = 0.903 and plotted these calculated points in Fig. 1a. The agreement with the ^{40}Ar,2np reaction product ^{211}Bi is now within the experimental resolution, which is all that can be expected from such a crude model.

Several mechanisms were considered to explain the large discrepancy between the calculated and observed 3n cross section, among them: precompound evaporation effects, enhanced tunneling, possible shell effects in the reaction mechanism, superfluidity, pairing effects and others. The most satisfying interpretation however is based on an angular momentum balance, and can best be visualized in the grazing-collision (GC) picture. For a detailed description see Klapdor et al.[13] In Fig. 3 we have applied this model to the $^{48}Ca + ^{208}Pb \rightarrow ^{256}No^*$ reaction, showing the "maximum" orbital angular momentum (J_{max}) which can be brought in by the ^{48}Ca for two excitation energies (30 and 40 MeV) and the maximum angular momentum which can be removed by the 2n-pseudo-particle. As demonstrated in many examples in Refs. 13-16, the maximum cross sections of the reactions lie within the inverted parabola(s) (Fig. 3). The vertex of the "half parabola" defined by L_{in}^{graz} and L_{out}^{graz} is given by $E = E_P^{cm} + Q - V_c$ with E_p^{cm} the projectile energy in the center of mass system, Q the Q-value, and V_c the coulomb barrier in the exit channel. For evaporation neutrons E is equal to excitation energy of the compound nucleus. In heavy-ion reactions the angular momentum brought in by the projectile cannot be larger than the critical angular momentum. This is the case for the GC-curve associated with E = 30 MeV (E_p^{cm} = 184 MeV) Fig. 3, where the critical angular momentum as calculated[17] from

$$J_{crit} = \left(\frac{\sigma_{CF}^{(mb)} A_p A_T \cdot E_p^{cm}}{651.23(A_p + A_T)} \right)^{1/2} \qquad (3)$$

is 30 ħ† while L_{Ca}^{graz} is 53 ħ. For the case of E = 40 MeV (E_p^{cm} = 194 MeV) the maximum angular momentum is determined by the grazing limit (L_{Ca}^{graz} = 82 ħ).

We now consider the de-excitation process of the compound nucleus which can in principle proceed via the emission of neutrons, charged particles, γ-rays, or all three. The minimum level to which the nucleus can de-excite at a given angular momentum is determined by the yrast line E(J). The yrast line for ^{256}No was scaled from measured values for ^{238}U,[18] assuming an $A^{5/3}$ dependence; specifically E(J) = 5.43 J^2(keV)††. The region important for γ decay ("γ-cascade band")

---

† The complete-fusion cross section σ_{CF} in Eq. 3 was obtained from the JORPL calculations adjusted to reproduce the experimentally determined 2n cross section.

†† This expression might not be correct at higher J values where the moment of inertia approaches the rigid-rotor value.[19] This is indicated in Fig. 3 by the curve labeled $E(J)_{rr}$.

is located between the yrast line and a line drawn approximately one neutron binding energy above and labeled $k_\gamma = 0.5$. Within a few tenths of an MeV below the $k_\gamma = 0.5$ line γ decay takes over almost completely and becomes the main de-excitation process.[20]

A more detailed study of Fig. 3 reveals that $2n\gamma$ is the main exit channel for the ^{48}Ca on ^{208}Pb reaction; charged-particle emission is completey prohibited. The GC curves for protons and alpha particles (labeled L_p^{graz} and L_α^{graz}) are below the yrast line. (Our experimental limits are $\sigma(^{48}Ca,p) \leqq 0.4$ μb and $\sigma(^{48}Ca,\alpha) \leq 0.7$ μb.) The $^{48}Ca,1n$ reaction is suppressed because the minimum excitation energy is 26 MeV. (Our experimental limit for ^{255}No is 35 nb.) After the evaporation of two neutrons almost all de-excitation channels terminate within the γ-cascade band. Thus a 3n process is possible for only a small fraction of the complete fusion cross section at the highest excitation energy as indicated by the ratio σ/σ_{max}, the horizontal bar at $E^* = 40$ MeV in Fig. 3 (here $\sigma/\sigma_{max} = \sigma_{CF}^{J}/\sigma_{CF}^{J=max}$). The larger-than-calculated width of the 2n excitation function could be related to this effect: the 2n channel continuing to dominate at increasing excitation energies due to the rising yrast line.

The authors are grateful to Drs. N. K. Glendenning and F. S. Stephens for inspiring discussions.

REFERENCES

* This work was done with support from the U. S. Energy Research and Development Administration.

1. E. K. Hulet, R. W. Lougheed, J. F. Wild, J. H. Landrum, P. C. Stevenson, A. Ghiorso, J. M. Nitschke, R. J. Otto, D. J. Morrissey, P. A. Baisden, B. F. Gavin, D. Lee, R. J. Silva, M. M. Fowler, G. T. Seaborg, to be published in Physical Review Letters.
2. W. D. Myers and W. J. Swiatecki, UCRL-11980 (1965).
3. A. Ghiorso, J. M. Nitschke, J. R. Alonso, C. T. Alonso, M. Nurmia, G. T. Seaborg, E. K. Hulet, R. W. Lougheed, Phys. Rev. Lett. 33, 1490 (1974).
4. J. M. Nitschke, Nucl. Inst. Meth. 138, 393 (1976).
5. B. F. Gavin, IEEE Transactions on Nucl. Science NS-23, 1008 (1976).
6. J. R. Alonso, Gmelin: Handbuch der Anorganischen Chemie, 7b, 28 (1974).
7. Yu. Ts. Oganessian, Yu. P. Tretyakova, A. S. Iljinov, A. G. Demin, A. A. Pleve, S. P. Tretykova, V. M. Plotko, M. P. Ivanov, N. A. Danilov, Yu. S. Korotkin, N. G. Glerov, JINR D7-8099 (1974).
8. K. E. Williams, private communication.
9. G. N. Flerov, Yu. Ts. Oganessian, A. A. Pleve, N. V. Pronin, Yu. P. Tretyakov, JINR D7-9555 (1976).
10. Atomic Data and Nucl. Data Tables 17, 411 (1976).
11. R. Hofstadter, Ann. Rev. Nucl. Sci., 7, 231 (1957).
12. J. Błocki, J. Randrup, W. J. Swiatecki, C. F. Tsang, LBL-5014, to be published in Ann. of Physics 1977.

13. H. V. Klapdor, G. Rosner, H. Reiss, M. Schrader, Nucl. Phys. A244, 157 (1975).

14. H. V. Klapdor, H. Reiss, G. Rosner, M. Schrader, Phys. Lett. 49B, 431 (1974).

15. H. V. Klapdor, H. Willmes, Phys. Lett. 62B, 395 (1976).

16. H. V. Klapdor, H. Reiss, G. Rosner, Nucl. Phys. A262, 157 (1976).

17. S. Cohen, F. Plasil, W. J. Swiatecki, Ann. of Phys. 82, 557 (1974).

18. E. Gross, J. deBoer, R. M. Diamond, F. S. Stephens, P. Tjøm, Phys. Rev. Lett. 35, 565 (1975).

19. F. S. Stephens, private communication.

20. J. R. Grover, J. Gilat, Phys. Rev. 157, 814 (1967).

FIGURE CAPTIONS

Fig. 1. Measured and calculated (dashed lines) excitation functions for the reaction $^{208}Pb(^{40}Ar,Xn)^{258-X}$ Fm (a) and $^{208}Pb(^{48}Ca,Xn)^{256-X}No$ (b) and associated transfer reactions. The curve drawn through the solid dots (Fig. 1a) is calculated from ^{48}Ca on ^{208}Pb results (see text).

Fig. 2. Interaction potential V(r) for ^{40}Ar on ^{208}Pb (a) and ^{48}Ca on ^{208}Pb for different values of angular momentum (b).

Fig. 3. Grazing-collision picture for the reaction $^{208}Pb(^{48}Ca,2n)^{254}No$ for two different excitation energies (30 Mev and 40 Mev) with yrast line E(J), cascade band limit $k_{\gamma} = 0.5$, and rigid-rotor calculation of the yrast line $E(J)_{rr}$. The horizontal bars at E* = 30 and 40 MeV indicate the fraction of the total fusion cross section as a function of J in a sharp cut-off model.

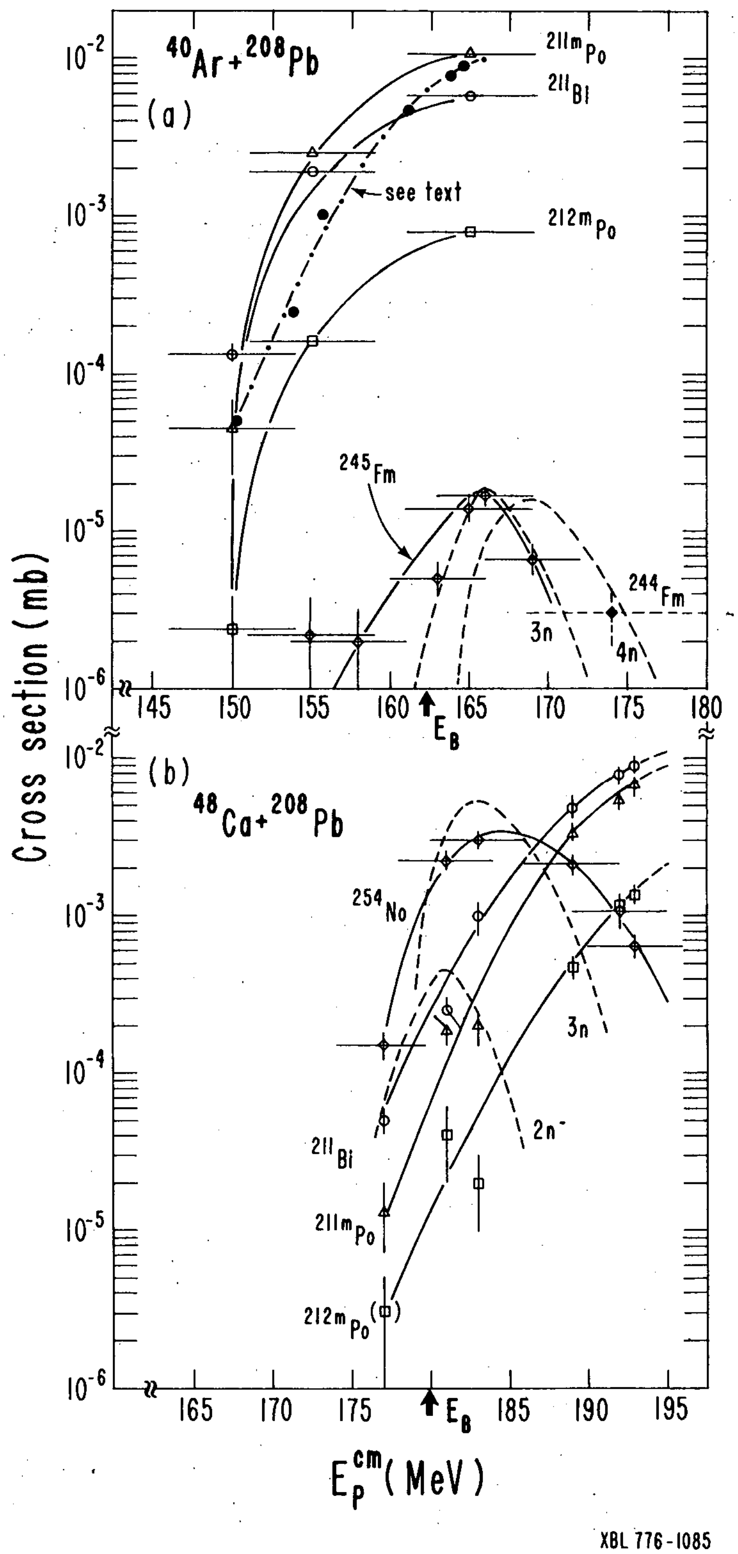

$^{40}Ar + ^{208}Pb$
(a)
^{211m}Po
^{211}Bi
see text
^{212m}Po
^{245}Fm
^{244}Fm
3n
4n
145 150 155 160 165 170 175 180
E_B
(b)
$^{48}Ca + ^{208}Pb$
^{254}No
3n
2n
^{211}Bi
^{211m}Po
^{212m}Po
165 170 175 180 185 190 195
Cross section (mb)
E_P^{cm} (MeV)
XBL 776-1085

Fig. 1

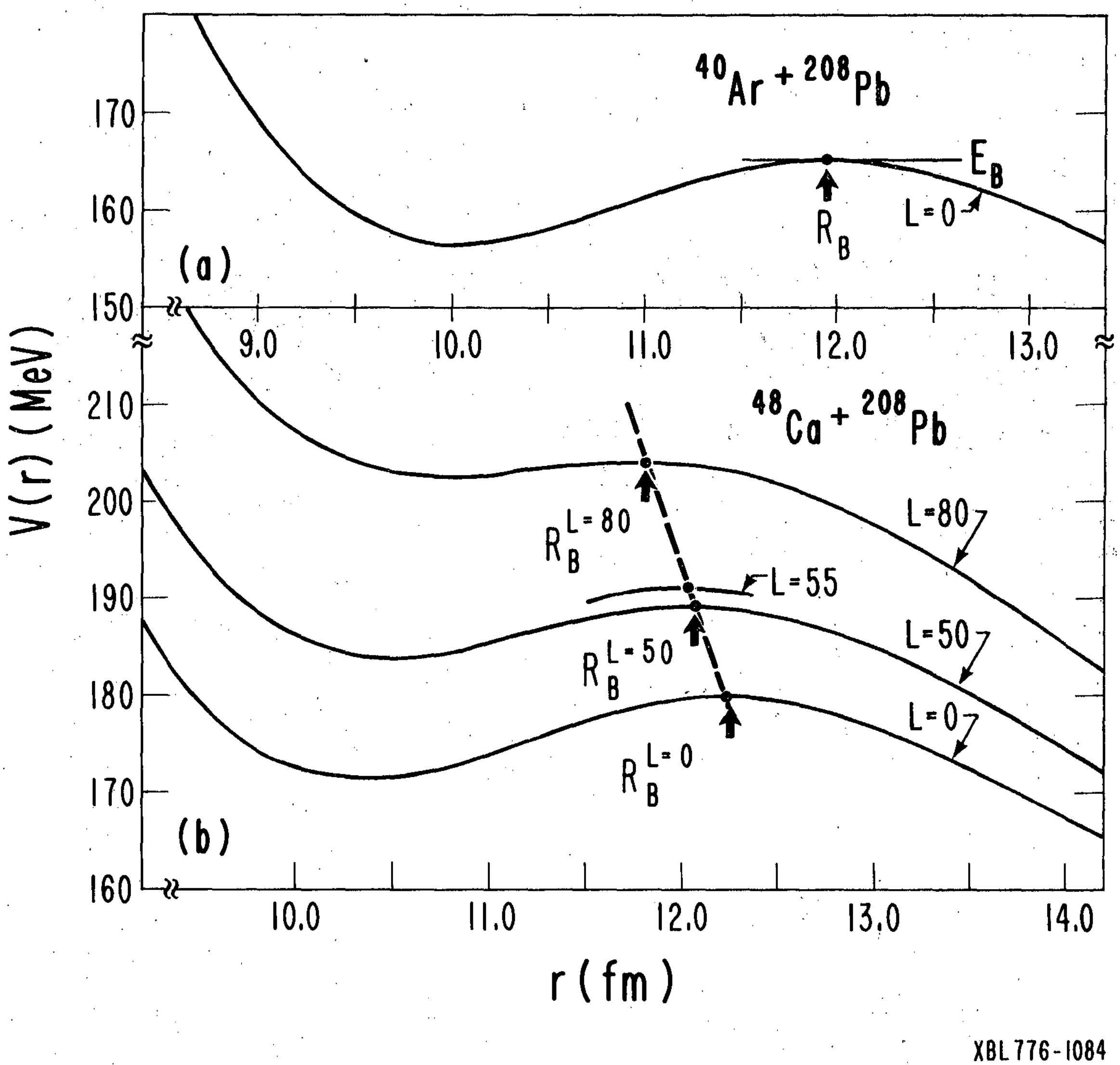

$^{40}Ar + ^{208}Pb$
E_B
R_B
L=0
(a)
170
160
150
9.0
10.0
11.0
12.0
13.0
V(r) (MeV)
$^{48}Ca + ^{208}Pb$
210
200
190
180
170
160
$R_B^{L=80}$
L=80
L=55
$R_B^{L=50}$
L=50
L=0
$R_B^{L=0}$
(b)
10.0
11.0
12.0
13.0
14.0
r (fm)
XBL 776-1084

Fig. 2

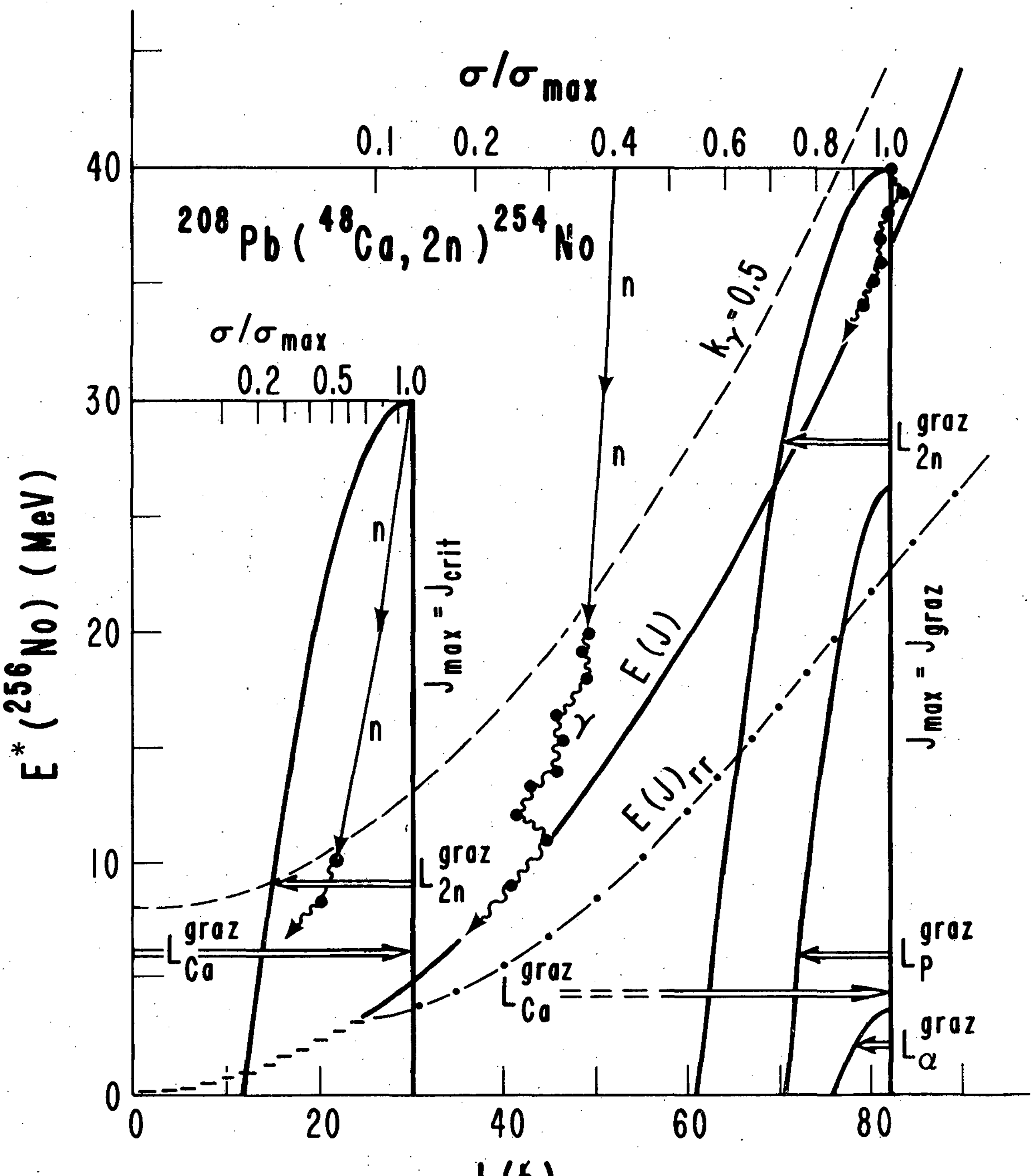

σ/σmax
0.1
0.2
0.4
0.6
0.8
1.0
208Pb(48Ca,2n)254No
n
kγ=0.5
σ/σmax
0.2
0.5
1.0
n
n
n
n
Jmax = Jcrit
γ
E(J)
E(J)rr
L2n graz
L2n graz
LCa graz
LCa graz
Lp graz
Lα graz
Jmax = Jgraz
E*(256No) (MeV)
J (ħ)
0
10
20
30
40
0
20
40
60
80
XBL 776-1083

Fig. 3

This report was done with support from the United States Energy Research and Development Administration. Any conclusions or opinions expressed in this report represent solely those of the author(s) and not necessarily those of The Regents of the University of California, the Lawrence Berkeley Laboratory or the United States Energy Research and Development Administration.

TECHNICAL INFORMATION DIVISION
LAWRENCE BERKELEY LABORATORY
UNIVERSITY OF CALIFORNIA
BERKELEY, CALIFORNIA 94720